Preparation of CQDs with hydroxyl function for Fe^{3+} detection

Limin Dong[1,2] ✉, *Wanqi Zhang*[1], *Xuejiao Li*[1], *Xiaoyao Geng*[1]

[1]*Heilongjiang Department of Education, College of Materials Science and Engineering, Harbin University of Science and Technology, Harbin, People's Republic of China*
[2]*Key Laboratory of Engineering Dielectrics and its Application, Ministry of Education, Harbin University of Science and Technology, Harbin, People's Republic of China*
✉ *E-mail: donglimin@hrbust.edu.cn*

Published in Micro & Nano Letters; Received on 6th July 2018; Revised on 6th December 2018; Accepted on 21st December 2018

Owing to its excellent fluorescence stability, unique up-conversion fluorescence properties and biocompatibility, carbon-quantum dots (CQDs) have become a research hot spot in the field of carbon materials. This study used a series of different preparation strategies to synthesise CQDs such as microwave method, solvothermal method and hydrothermal method. The prepared quantum dots can be further applied to design and metal ion detection. It is worth noting that the CQDs prepared by the hydrothermal method are evenly distributed in the range of 2–3 nm without any agglomeration. Fluorescence quenching was performed by Fe^{3+}, and the introduction of PO_4^{3-} ion could increase the fluorescence intensity of CQDs-Fe^{3+} system. Furthermore, CQDs were hydroxyl functionalised by treating with ethanol. The functionalised CQDs synthesised by solvothermal method greatly enhanced the fluorescence intensity.

1. Introduction: Carbon nanomaterials play an important role in nanoscience due to their superior properties. These special properties make them widely used in composite materials, energy storage and conversion, sensors, drug delivery, field emission devices and nanoscale electronic components [1–8]. Carbon-quantum dots (CQDs) are a new class of carbon nanomaterials. CQDs are a group of carbon nanoparticles with a diameter of <10 nm [9]. They are rich on the surface of various organic functional groups. The performance and other advantages have attracted the attention of people in the material industry. CQDs have high solubility, chemical inertness, good biocompatibility, excellent fluorescence stability, excellent catalytic performance, adjustable emission wavelength and good up-conversion fluorescence characteristics [10–13].

Therefore, the method of synthesising CQDs has been continuously developed. In 2006, Sun *et al.* [7] discovered and first named 'carbon dots' in the process of laser ablation of graphite target experiments, namely 'CQDs'. Since then, various methods to synthesise CQDs were developed increasingly such as pyrolysis method [14], combustion method [15], hydrothermal/solvothermal method [16, 17] and microwave method [18]. At the same time, the stepwise optimisation of the synthesis method made CQDs rich in surface functional groups. These new CQDs could be applied to the sensitive detection of metal ions such as Fe^{3+} [19, 20], Hg^{2+} and Sn^{2+}. In this Letter, we synthesised CQDs by different methods and detected Fe^{3+} in an aqueous solution with high sensitivity and selectivity. The hydroxyl functionalised CQDs have good hydrophilicity and biocompatibility. In our Letter, we synthesised CQDs by different methods compared with the morphology of CQDs and detected Fe^{3+} with CQDs. The CQDs showed superior properties after functionality with hydroxyl groups. Comparing to methods that were reported [21], we chose different solvents to explore the best fluorescence performance of hydrothermal methods.

2. Materials and methods

2.1. Materials: Glucose ($C_6H_{12}O_6$, AR) were purchased from the Tianjin Zhiyuan Chemical Reagent Co. Ltd., China. Citric acid ($C_6H_8O_7 \bullet H_2O$, AR) and hydrogen peroxide (H_2O_2, AR) were obtained from the Tianjin Bodi Chemical Reagent Co. Ltd., China. Polyethylene glycol [$HO(CH_2CH_2O)_nH$, AR] and isopropanol were obtained from the TianJin Guangfu Chemical Reagent Co. Ltd., China. Ethanol (C_2H_5OH, AR) were purchased from the Tianjin Tianli Chemical Reagent Co. Ltd., HO (CH_2CH_2O, AR) nH were obtained from the Tianjin Kwangfu Institute of Fine Chemicals, China. All chemicals were analytical reagents, so they could be used directly without further purification.

2.2. Preparation: CQDs synthesised by the microwave, hydrothermal method and solvothermal method.

Microwave method: Glucose was dissolved in deionised water and mixed with 400 Da Polyethylene glycol (PEG-400) intensively by magnetic stirrers. After doing ultrasonic treatment for 1 h, the mixture was heated by a microwave oven at a certain power (300, 500, 800 and 1000 W) for a period of time (1, 2, 3, 4 and 5 min) to determine the best conditions, then put the mixture in a regenerated cellulose (RC) cellulose dialysis bag to obtain a CQD solution.

Hydrothermal method: Glucose was dissolved in deionised water, and the solution then formed a transparent solution under magnetic stirring for 30 min. After doing ultrasonic treatment for 30 min, the above mixing solution was transferred into a teflon-lined stainless steel autoclave and sealed, maintained at a certain temperature (100, 150, 200 and 250°C) for a period of time (6, 8, 10 and 12 h). The CQDs were collected by centrifugation.

Solvothermal method: Citric acid was dissolved in deionised water, *n*-propanol, ethanol and isopropanol. After doing ultrasonic treatment for 30 min, the above mixing solution was transferred into a teflon-lined stainless steel autoclave and sealed, maintained at 180°C for 12 h.

2.3. Characterisation: The phase of the product was identified by X-ray diffraction (XRD, PANalytical X'Pert PRO MPD, Holland) with copper (Cu)-Kα radiation ($\lambda = 0.154056$ nm). Morphological features of the samples were observed using field emission scanning electron microscopy (Sirion200, Philips) and transmission electron microscopy (TEM, JEM2100, Japan). Photoluminescence (PL, RF-5301PC, Shimadzu, Japan) spectra were measured at room temperature using a 150 W xenon lamp with a wavelength of 335 nm as the excitation source. Ultraviolet

© The Institution of Engineering and Technology 2019

doi: 10.1049/mnl.2018.5369

(UV)–visible spectra were recorded on a LengGuang UV757CRT spectrophotometer.

3. Result and discussion: XRD, TEM and Fourier-transform infrared spectroscopy (FT-IR) were used for analysing the structure and morphology. To determine the phase purity of the sample, XRD for the synthesised products were shown in Fig. 1. From the pattern of CQDs, a broad diffraction peak located at about 25° which belong to (002) crystal face. The amorphous characteristic peak shows that CQDs were not a continuous crystal structure. Therefore, CQDs, that we prepared, were amorphous carbon structure.

To detect the functional groups accurately and characterise the covalent bonding information of CQDs prepared by different methods, the FT-IR spectrum was shown in Fig. 2. There is no apparent difference of characteristic peaks between hydrothermal method and solvothermal method. The intense absorption peak at 3300 cm^{-1} was attributed to the stretching vibration of O–H. A peak at 1630 cm^{-1} indicated the stretching vibration of C = O. The presence of absorption peak at 540–565 cm^{-1} indicates bending vibration of C–O–C.

The morphological properties are essential properties for the crystal structure. TEM characterisation of the CQDs which were prepared by the hydrothermal reaction at 180°C for 12 h was obtained as shown in Fig. 3. From the high-resolution TEM photograph, we can see that the size of the prepared graphene quantum dots is about 2–3 nm; it proves that the particle is close to the zero-dimensional state. At the same time, it can be observed that the (002) crystal lattice fringes of CQD are clear and the interplanar spacing is about 0.23 nm.

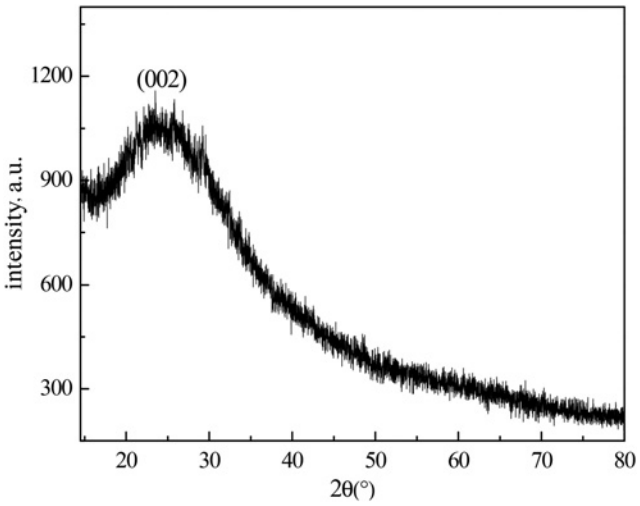


Fig. 1 *XRD pattern of CQDs*

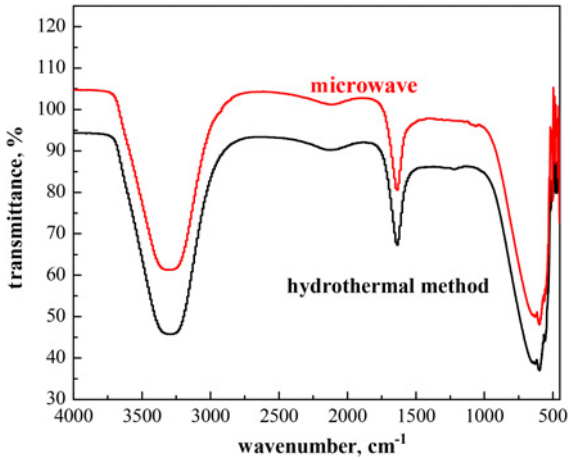


Fig. 2 *Infrared spectrum of CQDs prepared by hydrothermal and microwave methods*

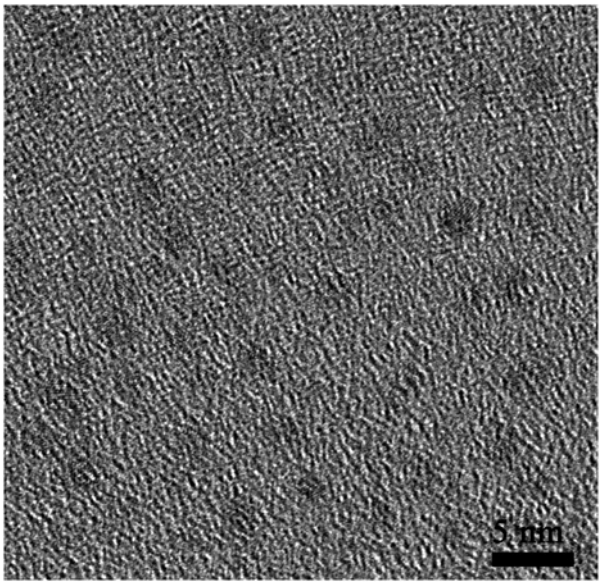


Fig. 3 *TEM micrographs of CQDs*

The spectrum of CQDs excited by the different excitation wavelengths at the range of 350–550 nm was shown in Fig. 4. Table 1 shows the recorded intensities for each excitation wavelength. When the excitation wavelength is 360 and 380 nm, the carbon dots exhibit the strongest fluorescence emission, and as the excitation wavelength is further increased, the fluorescence emission intensity of carbon dots begins to decrease. The maximum peak of fluorescence emission spectrum shifts to the longer wavelength with the increase of excitation wavelength. Combined with fluorescent photographs, excitation wavelength dependence was shown. With the increase of excitation wavelength, the fluorescence emission peak of carbon dots is red shifted, and the fluorescence colour is also shifted from short wavelength to long wavelength.

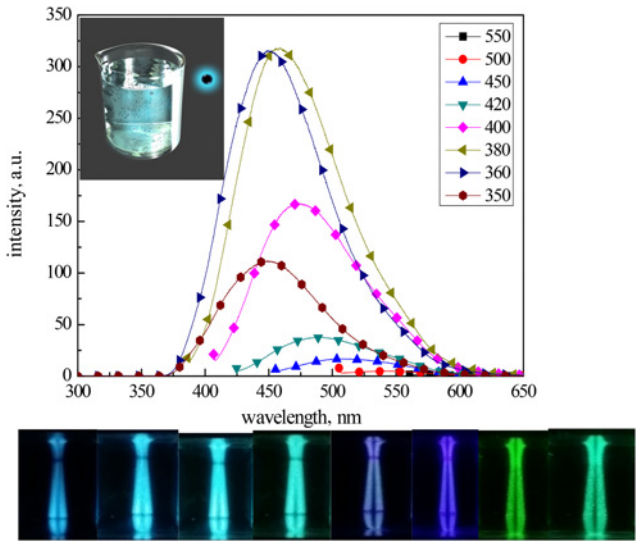


Fig. 4 *Fluorescence emission spectra of CQDs excited by different wavelengths and fluorescence photographs*

© The Institution of Engineering and Technology 2019

Table 1 Peak values of different curves

Wavelength, nm	350	360	380	400	420	450	500	550
intensity, a.u.	110.6	315.5	319.3	116.9	36.6	18.8	4.2	1.5

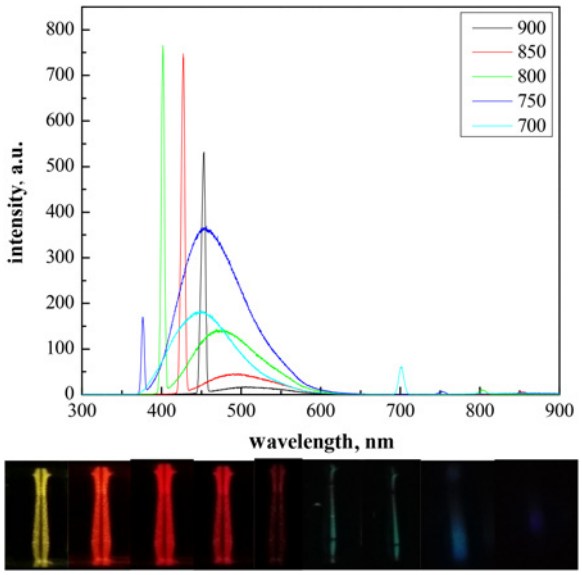


Fig. 5 *Fluorescence emission spectrum of CQDs excited by different wavelength and fluorescence photographs*

Table 2 Peak values of different curves

Wavelength, nm	700	750	800	850	900
intensity, a.u.	178.8	396.2	773.8	750.1	527.1

The spectrum of CQDs excited by the different excitation in the range of 700–900 nm was shown in Fig. 5 and peaks of different curves were shown in Table 2, which performed the change of intensity. When the excitation wavelength is increased from 700 to 900 nm, the carbon dots show an extremely obvious fluorescence emission peak in the range of 400–500 nm and the carbon dots emit blue fluorescence. When the excitation wavelength is increased from 700 to 750 nm, the fluorescence emission intensity of carbon dots gradually increases, and the fluorescence intensity begins to decrease with the further increase of the excitation wavelength. Fluorescence emission spectroscopy shows that CQDs not only have significant down-conversion fluorescence properties but also excellent up-conversion fluorescence properties.

The as-prepared CQDs have rich multifunctional groups, binding with metal ions has been reported. It was proved that CQDs had high sensitivity and selectivity of Hg^{2+}. As shown in Fig. 6, we determined to explore detection properties of CQDs for another heavy metal ion (Na, Ca, Zn, Mn, Cu, K, Ni, Mg and Fe) on the PL intensity of the reaction system (The concentrations of metal ions were 1 μM, the volume of the solution was 10 ml, and B was control group). With the addition of Zn, Ca, Na and K, the fluorescence intensity of CQD is enhanced. In contrast, the fluorescence quenching efficiencies of CQDs with Fe, Cu, Ni and Mn ions are shown as follows: Fe > Cu > Ni > Mn. It was indicated that the fluorescence of CQDs could be quenched by Fe^{3+} drastically. This is because CQDs are excited by light to generate multiple electron–hole pairs. When metal ions are added to the CQD solution, charge transfer occurs during light irradiation.

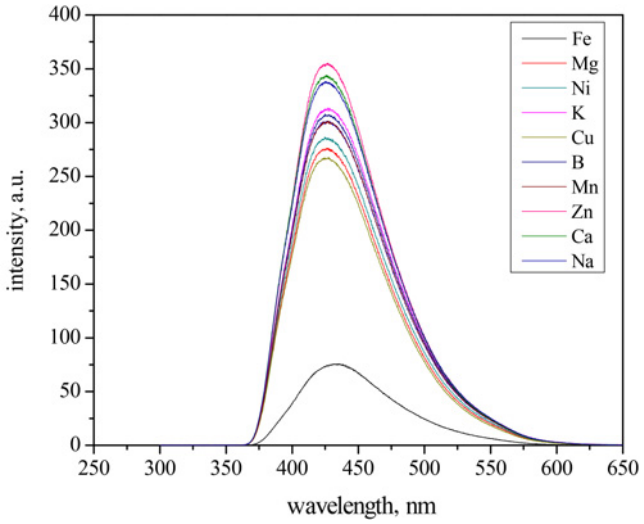


Fig. 6 *Influence of metal ions on CQDs fluorescence intensity*

We proposed that an inferred quenching mechanism through effective electron transfer process could promote non-radiative electron–hole complex quenching.

Owing to the excellent property of fluorescence quenching, CQDs could be used to detect Fe^{3+}. The different concentrations (1 μM, 2 μM, 3 μM, 4 μM and 5 μM) of Fe^{3+} influence the CQDs fluorescence intensity as shown in Fig. 7. With the increase of the concentration of Fe^{3+}, the fluorescence intensity of the CQDs was decreased. When the concentration of Fe^{3+} is 1 μM, the fluorescence quenching effect is worked obviously. The fluorescence intensity nearly disappeared when the concentration is above 2 μM. This was because of the interaction between Fe^{3+} and the hydroxyl groups on the surface of CDs as they were added to the system, which resulted in the aggregation of CDs and further resulted in fluorescence quenching. At the same time, the formation of precipitates also confirmed the formation of complexes.

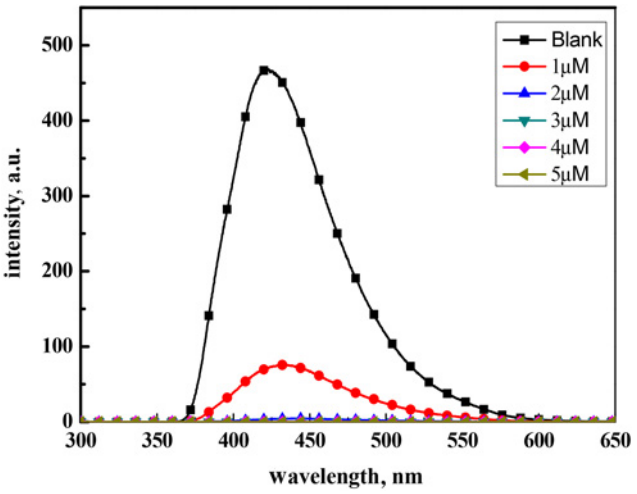


Fig. 7 *Effect of Fe^{3+} concentration on CQDs fluorescence intensity*

© The Institution of Engineering and Technology 2019

doi: 10.1049/mnl.2018.5369

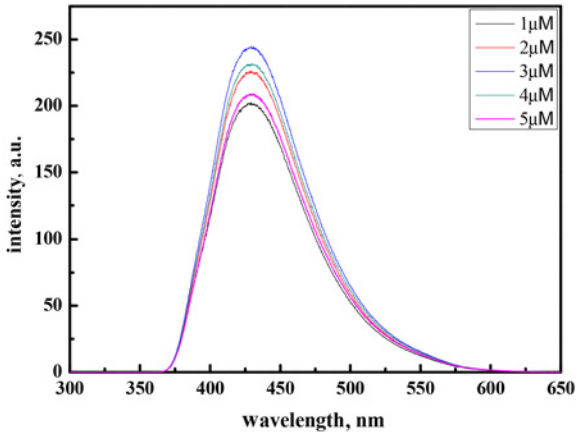


Fig. 8 *Fluorescence intensity of CQDs-Fe^{3+} system after H_3PO_4 addition*

After adding phosphoric acid (H_3PO_4) solution into the CQDs-Fe^{3+} system at the different concentrations (1, 2, 3, 4 and 5) of Fe^{3+}, the result of fluorescence intensity was shown in Fig. 8. The results show a significant increase in fluorescence intensity with concentrations above 2 M. Owing to the Fe–O bond interaction, the addition of PO_4^{3-} ions can improve the fluorescence intensity of the CQDs-Fe^{3+} system.

We plotted the fluorescence intensity histograms for the different systems. The fluorescence intensity of CQDs-Fe^{3+} system began to increase after the introduction of PO_4^{3-} ions, and precipitation of CQDs-Fe^{3+} system disappeared. After adding PO_4^{3-} ions, the pH of CQDs-Fe^{3+} system was 3, the analysis shows that the fluorescence intensity of CQDs solution is not high under strong acid environment. Therefore, by controlling the amount of H_3PO_4 to control the pH value of CQDs-Fe^{3+} system, the fluorescence intensity can be further improved. The introduction of PO_4^{3-} ions can increase the fluorescence intensity of CQDs-Fe^{3+} system because of the interaction between $PO4^{3-}$ ions and Fe^{3+} ions through the Fe–OP bond. Therefore, CQDs-Fe^{3+} system can also be used as a fluorescent probes detector for detecting PO_4^{3-} ion. Fig. 9 showed the interaction of PO_4^{3-} ions with CQDs-Fe^{3+} system.

To observe the difference between CQDs and hydroxyl functionalisation of CQDs, FT-IR spectra were shown in Fig. 10. C–H stretching vibration peak was observed around 3085 cm^{-1}, and around the 804–898 cm^{-1} the in-plane bending vibration peak of C–H in the 1779 cm^{-1} appearing. The peak at 1400 cm^{-1} belonged to the bending vibration peak of O–H and 1196 cm^{-1}

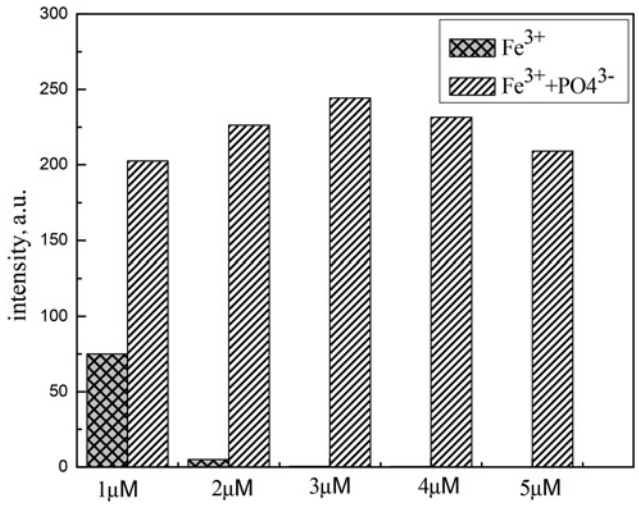


Fig. 9 *Fluorescence intensities of CQDs-Fe^{3+} and CQDs-Fe^3/PO_4^{3-} systems*

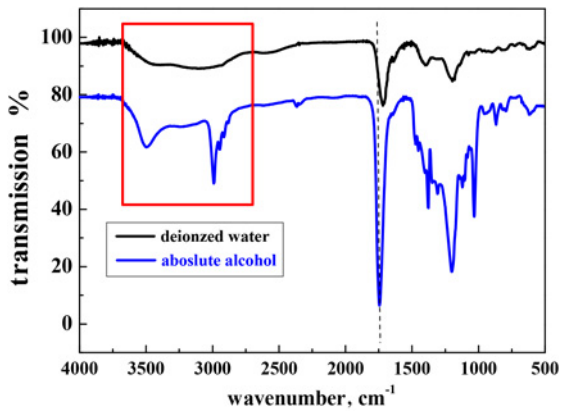


Fig. 10 *FT-IR of CQDs prepared by different methods*

is due to the C–O stretching vibration peak, while the stretching vibration peak of C–O–C appears around 1075 cm^{-1}.

The absorption peak around 2984 cm^{-1} belonged to the stretching vibration peak of C–H, and the absorption peak around 1738 cm^{-1} belonged to the vibration peak of –COOH as the dotted line. The absorption peak at 1400 cm^{-1} belongs to the stretching vibration peak of –OH, and the vibration peak around 1195 cm^{-1} belongs to the C–O stretching vibration peak, and the absorption peak of the C–H inward bending vibration peak exists at 784–857 cm^{-1}.

Compared to the infrared visible absorption spectra of CQDs prepared by deionised water and anhydrous ethanol, we found that the solute-based solvothermal method for the preparation of CQD surface-rich group –COOH and –OH indicates that the solvothermally prepared CQDs have better water solubility than hydrothermally prepared CQDs. Meanwhile, comparing with graphene quantum dots were reported [22, 23], the CQDs that we prepared had richer functional groups.

Morphology of CQDs-OH is shown in Fig. 11. From these TEM images, we can observe that the prepared CQDs are uniform in size and approximately as spheres. Notably, the quantum dots had good dispersibility, no agglomeration, dense distribution and high quantum yield. It was shown that the sizes of the prepared CQDs were between 2 and 3 nm, which is close to the zero-dimensional size.

The PL spectra of CQDs were prepared under the condition that the temperature and time of the insulation were consistent. The excitation wavelength was 380 nm. The curve 12a shows the PL curve of CQDs prepared with deionised water as the solvent, with the strongest emission peak at 456 nm. The curve 12b was the PL curve of the CQDs prepared from isopropanol. The emission peak position was 450 nm. The 12c curve was the PL curve of CQDs prepared in *n*-propanol. The emission peak position

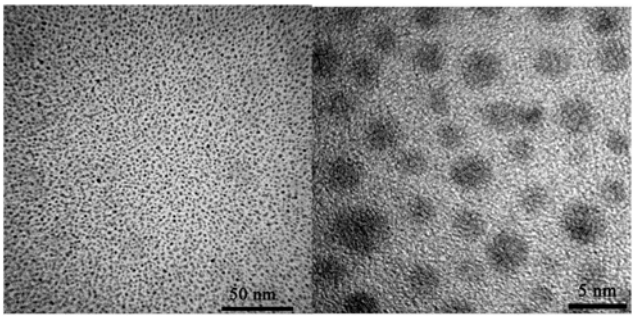


Fig. 11 *TEM of CQDs-OH*

© The Institution of Engineering and Technology 2019

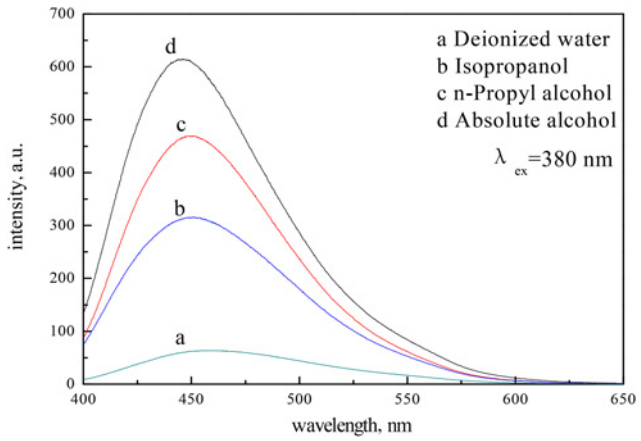


Fig. 12 *PL spectra of CQDs prepared by different solvents*

was 450 nm. The curve 12d was the strongest PL curve from the preparation of CQDs from anhydrous ethanol.

In Fig. 12, the strongest emission peak was at 446 nm. It could be clearly seen that the PL effect of the CQDs prepared using absolute ethanol was the best and the luminescence intensity was the highest. Therefore, through the analysis of the results of PL, ethanol was selected as the solvent for the preparation of CQDs by solvothermal method.

4. Conclusion: In this Letter, we prepared CQDs by the ultrasonic-assisted solvothermal method and found that CQDs prepared by using absolute ethanol as solvent have the best application potential by optimising experimental conditions successfully. The most suitable soaking temperature is 180°C, and the optimum soaking time is 12 h. By comparing the PL properties of different excitation wavelengths, we found that CQDs also showed remarkable excitation wavelength dependence and excellent up-conversion characteristics. The CQDs prepared by the method have a uniform diameter distribution of about 2–3 nm, and the surface of the CQDs is rich in hydroxyl and carboxyl functional groups. This means that the functionalised CQDs have good hydrophilicity and biocompatibility, and have great application potential in the life science and biomedical fields. Fe^{3+} can interact with polar amino groups and oxygen-containing groups on the surface of CQDs. The chelation reaction is initiated by non-radiative quenching and the photogenerated electrons in the excited state are deactivated, which means that the carbon dots can be used to detect Fe^{3+} in the aqueous solution with high sensitivity and selectivity.

5. Acknowledgments: This work was financially supported by the Natural Science Foundation of Heilongjiang Province (grant no. QC2017056) and the Harbin Scientific and Technological Innovation Talent Fund (grant no. 2016RQXXJ054).

6 References

[1] Yuan F., Li S., Fan Z., *ET AL.*: 'Shining carbon dots: synthesis and biomedical and optoelectronic applications', *Nano Today*, 2016, **11**, (5), pp. 565–586

[2] Lyu S., Chen Y., Han S., *ET AL.*: 'Layer-by-layer assembled polyaniline/carbon nanomaterial-coated cellulosic aerogel electrodes for high-capacitance supercapacitor applications', *RSC Adv.*, 2018, **8**, (24), pp. 13191–13199

[3] Liu Y.T., Pan L., Zhou Z.W., *ET AL.*: 'A universal strategy for the in-situ synthesis of TiO_2(B) nanosheets on pristine carbon nanomaterials for high-rate lithium storage', *J. Mater. Chem. A*, 2018, **6**, (16), pp. 7070–7079

[4] Larson D.R., Zipfel W.R., Williams R.M.: 'Water-soluble quantum dots for multiphoton fluorescence imaging in vivo', *Science*, 2003, **300**, (5624), pp. 1434–1436

[5] Lim S.Y., Shen W., Gao Z.: 'Carbon quantum dots and their applications', *Chem. Soc. Rev.*, 2015, **44**, (1), pp. 362–381

[6] Li H., He X., Kang Z.: 'Water-soluble fluorescent carbon quantum dots and photocatalyst design', *Angew. Chem., Int. Ed.*, 2010, **122**, (26), pp. 4532–4536

[7] Sun Y.P., Zhou B., Lin Y.: 'Quantum-sized carbon dots for bright and colorful photoluminescence', *J. Am. Chem. Soc.*, 2006, **128**, (24), pp. 7756–7757

[8] Hardman R.: 'A toxicologic review of quantum dots: toxicity depends on physicochemical and environmental factors', *Environ. Health Perspect.*, 2006, **114**, (2), pp. 165–172

[9] Baker S.N., Baker G.A.: 'Cheminform abstract: luminescent carbon nanodots: emergent nanolights', *Angew. Chem., Int. Ed.*, 2010, **49**, (38), pp. 6726–6744

[10] Shen J., Zhu Y., Yang X., *ET AL.*: 'Graphene quantum dots: emergent nanolights for bioimaging, sensors, catalysis and photovoltaic devices', *Chem. Commun.*, 2012, **43**, (29), pp. 3686–3699

[11] Tang L., Ji R., Cao X., *ET AL.*: 'Deep ultraviolet photoluminescence of water-soluble self-passivated graphene quantum dots', *ACS Nano*, 2012, **6**, (6), p. 5102

[12] Li Q., Ohulchanskyy T.Y., Liu R., *ET AL.*: 'Photoluminescent carbon dots as biocompatible nanoprobes for targeting cancer cells in vitro', *J. Phys. Chem. C*, 2010, **114**, (28), pp. 12062–12068

[13] Pan D., Guo L., Zhang J., *ET AL.*: 'Cutting sp2 clusters in graphene sheets into colloidal graphene quantum dots with strong green fluorescence', *J. Mater. Chem.*, 2012, **22**, (8), pp. 3314–3318

[14] Liu H., Ye T., Mao C.: 'Fluorescent carbon nanoparticles derived from candle soot', *Angew. Chem., Int. Ed. Engl.*, 2007, **46**, (34), pp. 6473–6475

[15] Bourlinos A.B., Stassinopoulos A., Anglos A., *ET AL.*: 'In surface functionalized carbogenic quantum dots', *APS Meet.*, 2008, **4**, (4), pp. 455–458

[16] Yang Y., Cui J., Zheng M., *ET AL.*: 'One-step synthesis of amino-functionalized fluorescent carbon nanoparticles by hydrothermal carbonization of chitosan', *Chem. Commun.*, 2012, **48**, (3), pp. 380–382

[17] Guo Y., Chen Y., Cao F., *ET AL.*: 'Hydrothermal synthesis of nitrogen and boron doped carbon quantum dots with yellow–green emission for sensing Cr(VI), anti-counterfeiting and cell imaging', *RSC Adv.*, 2017, **7**, (76), pp. 48386–48393

[18] Zhu H., Yang X.: 'In microwave synthesis of fluorescent carbon nanoparticles with electrochemiluminescence properties', *Chem. Commun.*, 2009, **1**, (34), pp. 5118–5120

[19] Liu H., Zhang Y., Liu J.H., *ET AL.*: 'Preparation of nitrogen-doped carbon dots with high quantum yield from *Bombyx mori* silk for Fe(III) ions detection', *RSC Adv.*, 2017, **7**, (80), pp. 50584–50590

[20] Ma C.B., Zhu Z.T., Wang H.X., *ET AL.*: 'A general solid-state synthesis of chemically-doped fluorescent graphene quantum dots for bioimaging and optoelectronic applications', *Nanoscale*, 2015, **7**, (22), p. 10162

[21] Wang Y., Hu A.: 'Carbon quantum dots: synthesis, properties and applications', *J. Funct. Mater.*, 2014, **2**, (34), pp. 6921–6939

[22] Chua C.K., Sofer Z., Šimek P., *ET AL.*: 'Synthesis of strongly fluorescent graphene quantum dots by cage-opening buckminsterfullerene', *ACS Nano*, 2015, **9**, (3), pp. 2548–2555

[23] Jankovský O., Nováček M., Luxa J., *ET AL.*: 'A new member of the graphene family: graphene acid', *Chem. Eur. J.*, 2016, **22**, (48), pp. 17416–17424

© The Institution of Engineering and Technology 2019

doi: 10.1049/mnl.2018.5369